

Mitigating belief projection in explainable artificial intelligence via Bayesian Teaching

Scott Cheng-Hsin Yang,^{1†*} Wai Keen Vong,^{2†} Ravi B. Sojitra,^{3†},
Tomas Folke¹, Patrick Shafto¹

¹Department of Mathematics and Computer Science, Rutgers University
101 Warren Street, Newark, NJ 07102, USA

²Center for Data Science, New York University
60 5th Ave, New York, NY 10011, USA

³Department of Management Science and Engineering, Stanford University

[†]Equal contribution.

*To whom correspondence should be addressed; E-mail: scott.cheng.hsin.yang@gmail.com.

Abstract

State-of-the-art deep-learning systems use decision rules that are challenging for humans to model. Explainable AI (XAI) attempts to improve human understanding but rarely accounts for how people typically reason about unfamiliar agents. We propose explicitly modelling the human explainee via Bayesian Teaching, which evaluates explanations by how much they shift explainees' inferences toward a desired goal. We assess Bayesian Teaching in a binary image classification task across a variety of contexts. Absent intervention, participants predict that the AI's classifications will match their own, but explanations generated by Bayesian Teaching improve their ability to predict the AI's judgements by moving them away from this prior belief. Bayesian Teaching further allows each case to be broken down into sub-examples (here saliency maps). These sub-examples complement whole examples by improving error detection for familiar categories, whereas whole examples help predict correct AI judgements of unfamiliar cases.

While Artificial Intelligence (AI) can help address socially-relevant problems [1, 2, 3], it is important for humans to be able to scrutinize AI decisions so we may audit, understand, and improve performance; indeed, this is legally mandated in certain contexts [4, 5]. The best performing AI algorithms use decision rules that feel alien to most humans [6], which impedes the adoption of such AI in high-leverage contexts, emphasizing the need for successful explanations that facilitate human understanding and prediction of the AI's behavior.

A popular class of methods to explain AI is *explanation-by-examples*. Explanation-by-examples takes as input an AI model to be explained and the data that it has been trained on and produces as output a small subset of training data that exert high impact on the inference of the explainee. For example, if the aim is to explain whether a deep-learning model would classify a given image as a

cat or a dog, explanation-by-examples selects the cat and dog images that are most representative of those categories. The utility of explanation-by-examples is supported by research that confirms humans' ability to induce principles from a few examples [7, 8, 9, 10] as well as the extensive use of examples in education [11, 12, 13]. The explanation-by-examples approach has many desirable properties: It is fully model-agnostic and applicable to all types of machine learning [14, 15, 16]; it is domain- and modality-general [17, 18]; and it can be used to generate both global explanation [19, 20, 21, 22, 23] and local explanation [24, 25, 26]. Although the technology of explanation-by-examples for XAI has been developed for at least two decades [27, 28], empirical tests and connections to its ecological roots in the social sciences have been limited.

Explanation-by-examples can be considered a social teaching act, which can be formally captured by *Bayesian Teaching* [29]. In Bayesian Teaching, there are two parties, a teacher (explainer) who selects examples and a learner (explainee) who draws inferences. The teacher selects examples intended to maximize the learner's probability of a correct inference based on the teacher's model of the learner's current beliefs and their inductive biases [30, 31, 32]; the learner uses Bayesian updating to make predictions given these examples [15, 33, 34, 35]. Existing work on explanation-by-examples has demonstrated explanation effectiveness relative to several baseline conditions [14, 20, 36, 37]; however, there is rarely a principled, *a priori* rationale as to why the proposed improvements should work. By explicating the computations used to model the explainer, the explainee, and the explanation selection process, Bayesian Teaching provides testable predictions on the effectiveness of explanatory examples in different contexts.

The core prediction of Bayesian Teaching is that explanations which lead the learner model to correct predictions will help humans to better understand the AI. By symmetry, explanations that lead the learner model to incorrect predictions will lead humans to targeted misunderstanding. Combining these, we hypothesize that the helpfulness of the examples positively covary with the predictive performance of the participants. We also hypothesize that participants prefer helpful examples over random examples, and that they prefer random examples over examples selected to be detrimental.

Because explanations generated by Bayesian Teaching is tailored to a learner model, it follows that explanation effectiveness depends on how accurately the explainee is modelled. We evaluate the fidelity of a learner model in the context of image classification. We use a popular deep-learning classifier as our model of the human explainee [38]. This is a reasonable starting point because such models effectively capture labels provided by humans, and as such encode some statistical patterns of human labelling. However, the way deep learning models learn from the Bayesian Teacher does not capture all human inductive biases. Below we suggest some potential sources of human bias and how they can be tested.

We expect that participants will treat predicting the AI as a social prediction task. In many social prediction tasks (in contrast to mechanistic prediction tasks) people use their own preferences or judgements as priors for other agents [39, 40, 41, 42, 43]. In our context that would mean participants projecting their own first-order beliefs onto the artificial agent, which results in a number of testable hypotheses outlined in the next paragraph.

Because humans generally perform well on image classification [44], they will expect the AI to be highly accurate, particularly for familiar categories; successful interventions would mitigate this expectation. In our experiment this would translate to humans who predict AI classification achieving higher sensitivity (correctly predicting AI's correct classifications) than specificity (correctly predicting AI's mistakes), absent explanation. Explanations, if effective, should re-

duce this difference by increasing specificity. Second, because unfamiliar categories have fuzzier mental representations, we hypothesize that examples improve predictive performance most for trials involving unfamiliar categories, and consequently that the preference for helpful examples is strongest when dealing with unfamiliar cases. Because more familiar categories should be easier to distinguish, and because participants expect the model to get the right answer for trials they themselves find easy, belief projection implies that *familiarity should increase predictive performance for model hits*. Conversely, *familiarity should decrease performance for model errors*. Finally, if explanations successfully shift participants away from belief-projection, they should mitigate these relationships between familiarity and performance.

The notion that humans model the AI as a social agent further implies that users would reason differently about AI’s correct classifications relative to its errors. Social priors tend to be “sticky” in that they are slow to update and are rarely completely overwhelmed by conflicting evidence [39, 45]. This stickiness may be driven by humans processing confirmatory and disconfirmatory evidence differently [46, 47]. The distinction between confirmatory and disconfirmatory evidence is currently not captured by our learner model, nor most other high-performing classification models, so if people make this distinction it has important implications for XAI. In our task we can test this by checking whether human performance and explanation effectiveness differ between trials where the aim is to confirm a correct prediction of the AI as opposed to detect a mistake.

An additional benefit of Bayesian Teaching is that it allows for selection of examples at different levels of granularity. For the current task, we consider the selection of entire images as well as pixels in an image as explanations. Surprisingly, the latter pixel-selection process derived from Bayesian Teaching turns out to be mathematically equivalent to a type of feature attribution method called Randomized Input Sampling for Explanations [48]. Thus the two levels of example granularity evaluated in this paper coincide with two popular methods of explanation—explanation-by-examples and saliency maps. We lack strong prior hypotheses for the relative impact of saliency maps and case-level examples, and how the two might interact. Consequently, we test a wide range of combinations and evaluate how they impact participants predictions of AI classifications.

We use image classification on *the ImageNet 1K dataset* [44] as the testbed. The model to be explained is ResNet-50 [38]. Following an ideal-observer approach [49, 50], we instantiate Bayesian Teaching by selecting examples with differing degrees of helpfulness as judged by the predictive performance of the learner model. For the learner model, we used a ResNet-50 model where the last softmax layer is replaced by a probabilistic linear discriminate analysis (PLDA) model. This alteration introduces the probabilistic training required by Bayesian Teaching while keeping the architecture of ResNet-50, which is known to accurately fit human labels [38]. The familiarity context is captured by ensuring that the categories selected cover a wide range of familiarity as judged by humans. The context of AI’s correct and mistaken predictions is straightforwardly manipulated by selecting test images that cover both cases. We also vary the informativeness of class labels (informative vs. generic) and how the saliency maps are presented (heatmap vs. blur) as additional contextual variables. Our investigation centered on the implications of Bayesian Teaching offers a comprehensive and nuanced picture of how explanations can mitigate belief projection in XAI.

Results

Methodological overview

User understanding in the context of classification can be captured by how well the user can predict the model’s judgement. Throughout this paper we will refer to this predictive capacity as performance. A natural measure of explanation effectiveness is how much the explanations increase such performance, relative to a control condition. We designed a two-alternative forced choice (2AFC) task in which participants were asked to predict the model’s classification of a target image between two given categories. No trial-by-trial feedback was provided to participants. It is important to note that in this task high performance does not imply that participants’ judgements match the ground truth of the image, which we refer to as first-order accuracy or simply accuracy. It is possible for a participant to have high accuracy (in that their judgements often match the ground-truth category of the image) but poor performance (in that their judgements rarely match the AI’s).

We designed a total of 15 conditions that vary along three dimensions: (1) presence of informative labels (two levels: [GENERIC LABELS] or ([SPECIFIC LABELS]), (2) types of examples (three levels: [NO EXAMPLES], [HELPFUL] or [RANDOM]), and types of saliency maps (three levels: [NO MAP], [JET] or [BLUR]). The labels dimension indicate whether the images shown were given informative labels (e.g. "Border terrier" or "Norwich terrier") or generic labels (Category A or Category B). The examples dimension indicate whether examples of the two image categories were shown, and if so, if they were selected to be helpful or were drawn from a uniform distribution of helpfulness as determined by Bayesian Teaching. The saliency map dimension indicates if the images were overlaid with saliency maps that highlighted which pixels the AI focused on to make its classification. If saliency maps were included, they were either visualized as a semi-transparent jet color map or as an image filter where unimportant pixels were blurred. We found no significant difference between the [BLUR] and [JET] conditions; thus, for increased clarity we use the [MAP] condition, which contains both variants, in the main text. See Supplementary Discussion D2 for the main analyses in the paper repeated with [BLUR] and [JET] coded separately. Table 1 shows the sample size of each condition. Figure 1 shows a trial where the categories are represented with informative label, helpful examples, and blur saliency maps.

		SPECIFIC LABELS			GENERIC LABELS	
		NO EXAMPLES	EXAMPLES			
			HELPFUL	RANDOM	HELPFUL	RANDOM
NO MAP		N = 76	N = 35	N = 34	N = 38	N = 36
MAP	BLUR	N = 65	N = 33	N = 36	N = 35	N = 34
	JET	N = 71	N = 33	N = 35	N = 35	N = 35

Table 1: Naming convention of conditions and the number of participants in each condition. In the main text, conditions are referred to with brackets and the “&” logical operation. For example, [NO EXAMPLES] & [NO MAP] refers to the condition with 76 participants (See Experimental conditions in Methods for more detail).

Each trial has three more distinct features beyond the condition it belongs to: the ResNet accuracy, the simulated learner performance, and a familiarity score. ResNet accuracy refers to the classification accuracy on the category which the target ResNet-50 model predicts that the target

On the right are two examples that belong to the category Flagpole, and two examples that belong to the category Barn. In addition, underneath each image are highlights indicating which parts of the image the robot is looking at to make its decision. Remember that the robot sometimes **makes mistakes**, so you should look at the examples closely to determine what the robot will do.







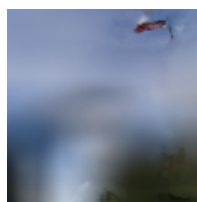
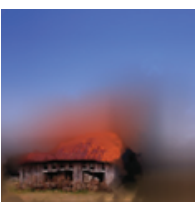
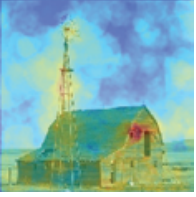
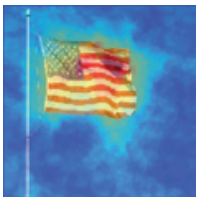
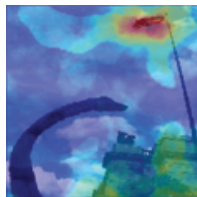


Target Image	Examples from Flagpole		Examples from Barn	
				
				
<p>Which category do you think the robot will classify the target image above as?</p> <p> <input type="button" value="Flagpole"/> <input type="button" value="Barn"/> </p>				
<hr/>				
				

Figure 1: A snapshot of the experiment. See Methods and Table 1 for the naming conventions of the conditions used below. The experimental condition above the black line is [SPECIFIC LABELS] & [HELPFUL] & [BLUR]. Under the black line is the [JET] equivalent of the second row, which is obtained by replacing the blurring maps with the jet color maps. Experimental conditions with generic labels are obtained by replacing specific labels—“Flagpole” and “Barn” in this case—with generic category names—“Category A” and “Category B.” Experimental conditions without the saliency maps, i.e., [NO MAP], show only the first row of images. Conditions without examples, i.e., [NO EXAMPLES], show only the first column of image(s). All images and saliency maps shown were 224-by-224 pixels. The prediction of the model to be explained on the target image is “Flagpole” in this case.

image belongs to (see Supplementary Table T1). Note that in contrast to the *ResNet accuracy* which is an accuracy on the category-level, we use the term *model correctness* to refer to whether the target model made a correct judgement on a specific trial. The simulated learner performance of a trial (only available in the [EXAMPLES] conditions) is an estimate of the probability that the learner model’s classification would match the target ResNet-50 model’s classification, given the categories and examples presented. Finally, in a separate study seven raters indicated their familiarity with each category pairing by stating whether they thought they could correctly match images of the two categories presented to their respective labels. The familiarity score is the mean

value across all seven raters. See the Methods for a more technical explanation of these features.

Bayesian Teaching improves predictive performance

To evaluate whether the XAI interventions improved human performance we compared participants who obtained a full explanation ([SPECIFIC LABELS] & [HELPFUL] & [MAP]) with a control group that received no explanations ([SPECIFIC LABELS] & [NO EXAMPLES] & [NO MAP]). When interpreting these results in relation to belief projection it is instructive to consider three idealized scenarios. An agent who picked categories at random would have 50% performance, sensitivity (correctly predicting AI classifications when the AI is correct), and specificity (correctly predicting the AI's mistakes). An agent who modelled the AI perfectly would have 100% performance, sensitivity, and specificity. Finally, an agent with perfect first-order accuracy who projected their own beliefs onto the AI would have 100% sensitivity, 0% specificity, and 33% overall performance because the experiment contains twice as many AI errors as AI correct classifications (see Methods). Absent intervention, participants behave most like the third, belief-projecting, agent (Figure 2).

The explanation interventions increase overall performance by increasing specificity (participants are better able to spot the AI's mistakes), at the cost of some sensitivity. Participants in the control condition have a mean performance of 49.83% [95% CI = 48.83% - 50.84%], significantly lower than the 55.04% [95% CI = 52.58% - 57.48%] performance of the experimental group ($\beta = 0.21(0.03)$, $z = 6.99$, $p < .0001$). This is primarily driven by higher specificity in the experimental group (43.98% [95% CI = 39.68% - 48.37%]) relative to the control group's 32.54% [95% CI = 30.96% - 34.13%]; $\beta = 0.49(0.05)$, $z = 9.20$, $p < .0001$). The greater vigilance of the experimental group came with a minor cost to sensitivity for the experimental group (78.90% [95% CI = 71.59% - 84.80%]) and for the control group (85.26% [95% CI = 83.12% - 87.22%]); $\beta = -0.43(0.12)$, $z = -3.68$, $p = .0002$), but not enough to offset the specificity gains. Collectively, these results imply that participants attempt to predict the AI by projecting their own beliefs, and that the explanations improve performance by mitigating this belief projection.

Participants prefer examples that are helpful according to Bayesian Teaching

Having established that examples generated by Bayesian Teaching improved participants' ability to predict AI judgements, we want to evaluate whether participants preferred helpful to random and misleading examples. To test this, we ran a second study where participants chose between helpful examples versus random examples or versus misleading examples, where helpfulness was determined by Bayesian Teaching. Participants showed a small but reliable preference for helpful relative to random examples and a substantial preference for helpful versus misleading examples. The preference for helpful examples was particularly pronounced when the image categories were unfamiliar to the participants (see Supplementary Discussion D1 for all the details).

Bayesian Teaching can lead participants to both correct and incorrect inference

Bayesian Teaching makes explicit the existence of an explainees and suggests that a sound learner model should have the capacity to track the inference of actual explainees. In our experiment the

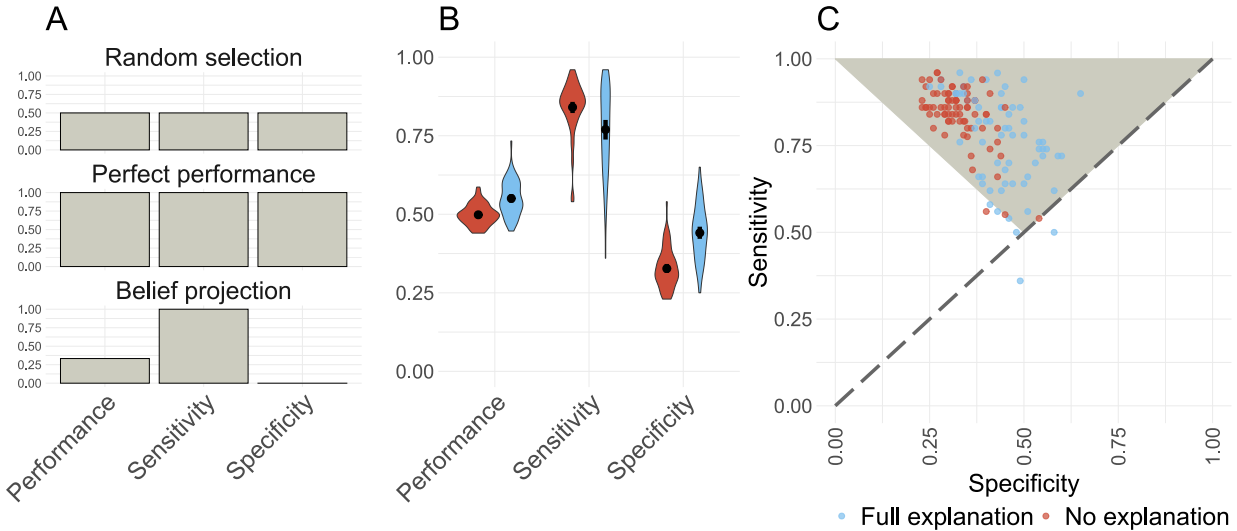


Figure 2: The effectiveness of examples generated by Bayesian Teaching, evaluated by comparing the performance of the participants who obtained a full explanation ([SPECIFIC LABELS] & [HELPFUL] & [MAP]; 66 participants; 9,899 observations) with a control group ([SPECIFIC LABELS] & [NO EXAMPLES] & [NO MAP]; 76 participants; 11,394 observations). (A). Three idealised performance profiles, showing the performance of: a random agent, a perfect agent, and an agent with perfect access to the ground truth who assumes that the AI always mirror their own predictions (belief projection). (B). Human performance most closely match the belief projection profile, but the interventions increase specificity (and slightly reduce sensitivity) by making participants better at spotting the AI’s errors. The violinplots show the distribution of performance within conditions. Black dots show the group mean with error bars signifying 95% bootstrapped confidence intervals. (C). Individual participants’ sensitivity and specificity. The vertices of the triangle show the performance of a belief-projecting agent with perfect access to the ground truth (upper left), an agent with a perfect model of the AI (upper right), and an agent choosing at random (lower middle). The control group is clustered at high sensitivity and low specificity towards the upper left, whereas the experimental group is shifted to the right. However, the experimental group also shows greater variance, signifying inter-individual differences in the intervention effectiveness.

calibration between the learner model and the participants is captured by the relationship between ResNet accuracy and participant accuracy. We estimate participant accuracy (their first-order belief about the ground truth) by using their performance in the control trials (their second-order belief about the AI with no exposure to explanation). The assumption that their attempt to predict the AI may serve as a proxy of their first-order accuracy is justified given the tendency to belief-project observed in previous sections. We found that participant performance (interpreted as accuracy for the control trials) was positively correlated with ResNet accuracy for trials where the model was correct ($\beta= 1.74(0.20)$, $z = 8.67$, $p < .0001$), indicating good calibration between the model and participants in this situation (see Supplementary Figure F1). We also found a negative interaction between ResNet accuracy and model correctness ($\beta= -2.57(0.23)$, $z = -11.03$, $p < .0001$). This suggests the poor calibration in the special case in which the model’s overall accuracy on the predicted category is high but it misclassifies the particular trial.

Bayesian Teaching should be able to modify participant performance by selecting explanations of varying helpfulness. To test this in practice, we ran three nested hierarchical logistic regression models of increasing complexity. Each regression model predicted participant performance (whether the participant correctly predicted the AI on a given trial) from the [EXAMPLES] trials only, as these are the only trials impacted by the simulated learner performance, which measures the degree to which the examples would lead the learner model to the targeted inference. The first regression model only included ResNet accuracy as a predictor as well as a dummy variable encoding whether the AI prediction for that trial matched the ground truth or not. The second regression model added simulated learner performance as a predictor. The third regression model added two two-way interactions between model correctness (model hit and error) and ResNet accuracy, and model correctness and simulated learner performance. We found that the second regression model fitted the performance data better than the first regression model ($\chi^2(1, 4) = 71.68, p < .0001$). This means that simulated learner performance predict participant performance above and beyond ResNet accuracy and whether the AI was correct for that specific trial. The third regression model outperformed the second regression model ($\chi^2(3, 7) = 7371.28, p < .0001$). This indicates that the predictive power of ResNet accuracy and/or simulated learner performance differed for trials with correct or incorrect AI judgements.

To explore how model correctness interacted with ResNet accuracy and simulated learner performance, we explored the parameters of the third regression model. Participants are typically better at predicting the AI when it is correct relative to when it is wrong ($\beta = 0.53(0.06), z = 9.15, p < .0001$). This aligns with our previous results, which suggest that participants have a sense of the ground truth for most trials, and assume that the AI would make the same judgement that they would make. ResNet accuracy is positively associated with participant performance when the AI is wrong ($\beta = 0.59(0.05), z = 12.30, p < .0001$), and even more strongly associated with performance when the AI is correct ($\beta = 0.93(0.09), z = 10.68, p < .0001$; see Figure 3). Because there was a significant positive relationship between ResNet performance for both the control trials and the example trials, it seems plausible that the calibration between model and participant observed in the control condition carries over to the example condition, at least partially. Finally, while statistically controlling for ResNet performance, simulated learner performance did not predict human performance on trials when the AI was wrong ($\beta = -0.01(0.03), z = -0.16, p = .89$) but did so for trials when the AI was correct ($\beta = 0.77(0.05), z = 14.19, p < .0001$). Because the simulated learner performance determined which examples were shown, the fact that this variable could accurately predict human performance above and beyond ResNet performance implies that the Bayesian Teacher can successfully shift the participant judgements in either direction.

Bayesian Teaching improves performance through belief-mitigation

The previous results indicate that examples improve participant predictions of the AI's classifications. Additionally, participants prefer examples that are helpful according to the Bayesian Teacher, and this preference is particularly pronounced for unfamiliar categories. Next, we will explore *how* explanatory examples improve performance, and evaluate the relative importance of the different explanation features employed. The preceding results imply that people belief-project by default: that is, they use their own beliefs as priors for the AI's beliefs. The interventions shift these priors, allowing the participants to distinguish their first-order beliefs about the correct classification from their second-order beliefs about the classifications of the AI.

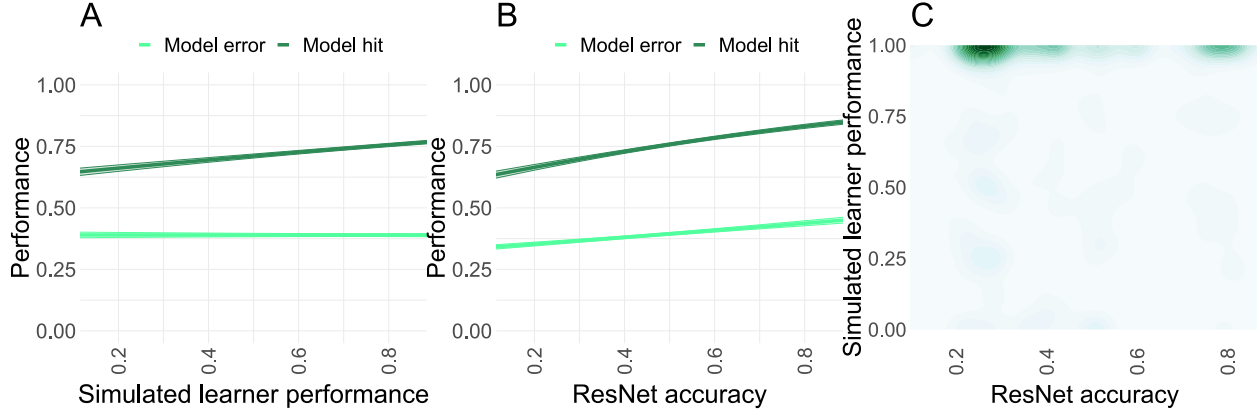


Figure 3: Simulated learner performance predicts human performance across trials with examples (419 participants; 62,820 observations). **(A)** The simulated learner performance—the helpfulness of the explanatory examples expected by the Bayesian Teacher—correlates significantly with participant performance for correct trials but not for incorrect trials. This suggests that the Bayesian Teaching framework can generate explanations that are informative or misleading for trials that are correctly classified by the model, but not for trials that are incorrectly classified. **(B)** ResNet accuracy is positively associated with participant performance, both for trials when the AI is correct and when it is wrong. A similar trend is observed in the control condition (see Supplementary Figure F1). This suggests that humans and ResNet find the same categories difficult to discriminate. The difference in performance between when the AI is correct and when the AI is wrong suggests that it is harder to teach incorrect judgements, at least in this context. **(C)** Two-dimensional kernel density with 25 density bins showing the distribution of trials in terms of ResNet accuracy and simulated learner performance. In this study the two are independent. Note that the higher density near perfect simulated learner performance was due to all the helpful examples being selected based on this variable, so they constitute a majority of our example trials.

To further evaluate whether explanations improve performance by mitigating belief-projection, we compared how the interventions impacted performance and first-order accuracy in the complete data set. Specifically we contrasted [SPECIFIC LABELS] vs [GENERIC LABELS], [MAP] vs [NO MAP], and [EXAMPLES] vs [NO EXAMPLES], while controlling for ResNet accuracy and familiarity score. We ran separate analyses for when the AI was correct and when the AI was wrong, corresponding to the distinction between sensitivity and specificity in previous sections. We will treat the ground truth as a proxy of participant first-order beliefs, an is defensible assumption given the reported human accuracy on ImageNet in previous works [44]. Based on this assumption, the interventions increasing performance while reducing the number of classifications that correspond to the ground-truth, would imply that the examples enable participants to move away from their first-order judgements. The [SPECIFIC LABELS] are associated with higher performance than the [GENERIC LABELS] regardless of whether the AI is correct ($\beta = 0.24(0.08)$, $z = 3.06$, $p = .002$) or not ($\beta = 0.07(0.03)$, $z = 2.13$, $p = .03$). However, because these effects are small and orthogonal to belief projection, they will not be discussed further.

The presence of the saliency maps in the [MAP] condition improves performance when the AI is wrong ($\beta = 0.43(0.03)$, $z = 14.24$, $p < .0001$), but reduces performance (to a lesser extent) when

the AI is correct ($\beta = -0.56(0.07)$, $z = -7.98$, $p < .0001$; see Figure 4). In both cases, saliency maps reduced the first order-accuracy of the participants (model hit: $\beta = -0.56(0.07)$, $z = -7.98$, $p < .0001$; model error: $\beta = -0.43(0.03)$, $z = -14.24$, $p < .0001$), meaning that they were less likely to report that they believed the AI's judgements matches the ground truth of the image. This implies that the saliency maps encourage participants to consider that the AI might be mistaken. One potential explanation for this observation is that the saliency maps show when the AI attends to non-sensible features (i.e. parts that are not representative of either of the categories) as well as ambiguous features (e.g. thin metal strips that are present in both the "Electric Fan" and "Buckle" category).

Comparing all [EXAMPLES] trials to all [NO EXAMPLES] trials, the presence of examples do not significantly improve performance when the AI is correct ($\beta = -0.13(0.08)$, $z = -1.61$, $p = .11$) or when the AI is wrong ($\beta = 0.02(0.03)$, $z = 0.69$, $p = .49$). However, in the conditions where examples were present, helpful examples improve performance for trials when the AI was correct ($\beta = 0.77(0.08)$, $z = 10.11$, $p < .0001$), but not for trials when the AI was wrong ($\beta = 0.06(0.04)$, $z = 1.77$, $p = .08$). The positive influence of the helpful but not the random examples confirms that Bayesian Teaching can shift beliefs from priors. Note that this is the opposite effect relative to what we found for the saliency maps: Whereas saliency maps help participants to identify trials when the AI has made a mistake by exposing sub-image-level features, the examples help reinforce participant's prior beliefs for trials in which the AI is correct (see Figure 4). In other words, the saliency maps and the examples serve separate and complementary functions in explaining AI judgements to the participants.

The familiarity scores capture the ease of the discrimination task in that they are higher for trials involving categories that humans are familiar with. These scores provide clues as to whether participants project their own beliefs onto the AI: If humans use their first-order classifications to model the AI, participants should assume that the AI gets the correct answer for trials that they themselves find easy. This is indeed what we find: familiarity is positively associated with performance when the and the AI is correct ($\beta = 1.10(0.04)$, $z = 29.28$, $p < .0001$), but negatively associated with performance for AI errors ($\beta = -0.92(0.02)$, $z = -42.82$, $p < .0001$; Figure 5).

Previously, we showed that saliency maps improved performance on trials when the AI was wrong. This could be explained by saliency maps helping participants distinguish between their first-order judgements of the ground truth and their second-order beliefs about the model classification. This explanation can be evaluated by testing whether the impact of the familiarity scores on performance are attenuated by the saliency maps. In other words, if participants are more likely to predict that the AI is correct on trials that they themselves find easy, and the saliency maps work by helping people realize that the AI use decision-processes that differ from their own, the saliency maps should make participants more willing to consider that the AI might be wrong for trials they themselves find easy. This is what we find (see Figure 5): the presence of saliency maps reduces the positive impact of familiarity on performance when the AI is correct ($\beta = -0.51(0.08)$, $z = -6.31$, $p < .0001$). Conversely, saliency maps reduce the negative impact of familiarity on performance when the AI is wrong ($\beta = 0.70(0.05)$, $z = 15.22$, $p < .0001$; Figure 5). Collectively these results suggest that the presence of saliency maps help participants model the AI as an agent with distinct beliefs that may conflict with their own.

Though the presence of examples did not generally impact performance, it is possible that they impacted judgements specifically for unfamiliar categories. Like the saliency maps, examples typically reduced the impact of familiarity on performance, both when the AI is correct ($\beta = -$

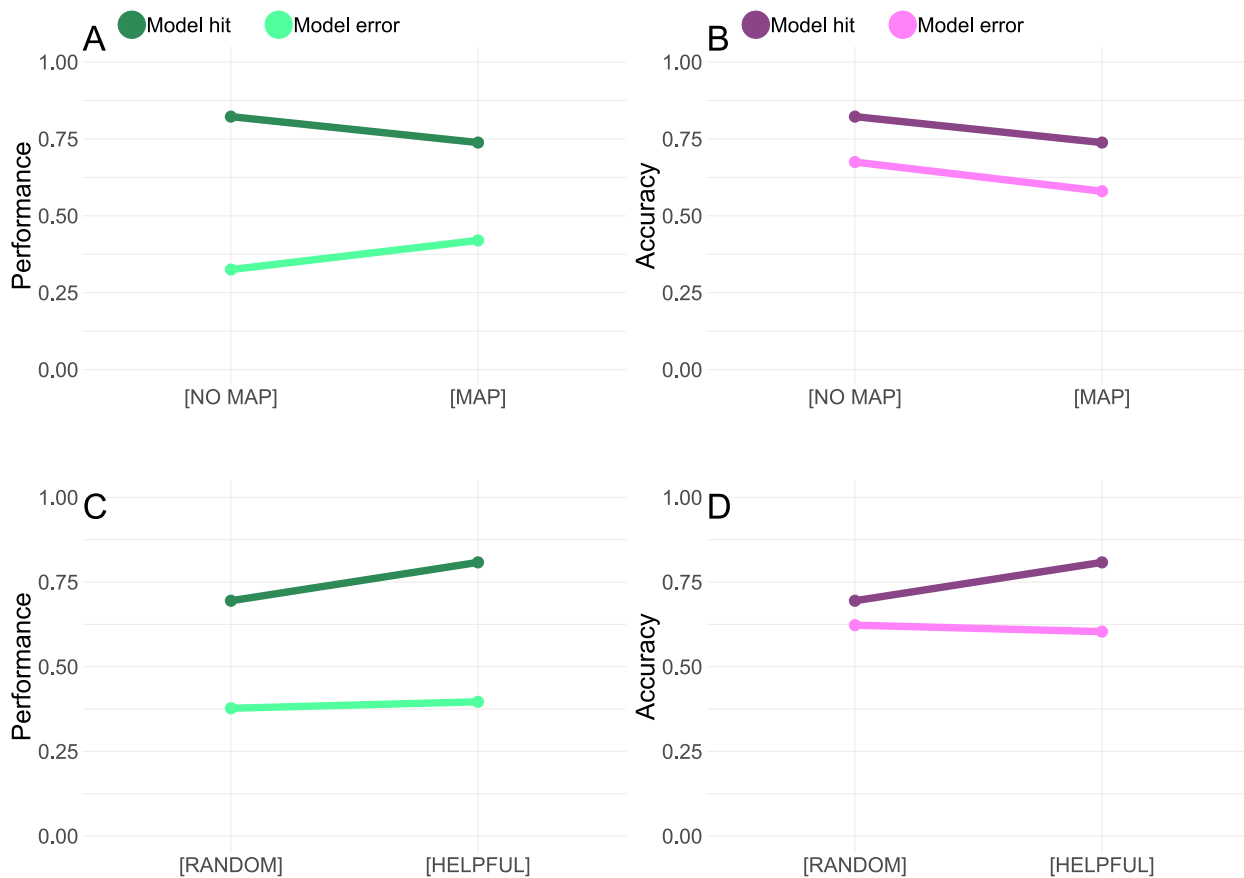


Figure 4: Task performance differs depending on AI classification accuracy. **(A)** & **(B)** are based on the entire data set, comparing all [MAP] conditions to all [NO MAP] conditions (631 participants; 94,582 observations). **(C)** & **(D)** exclude the [NO EXAMPLES] trials and contrast all [HELPFUL] trials with all [RANDOM] trials (419 participants; 62,820 observations). **(A)**. The saliency maps improve performance for trials when the AI is wrong but reduce performance when the AI is correct. **(B)**. The saliency maps make people less likely to classify the target image to align with the ground truth, independent of AI accuracy. Together, **(A)** & **(B)** imply that the saliency maps help people to consider that the AI might make mistakes. **(C)** In trials with examples, helpful examples tend to help people to accurately model the AI in cases when the AI is correct, but have a limited impact when the AI is wrong. **(D)** Consequently, helpful examples make participants more likely to pick the ground truth option when the AI is correct, but do not really impact the probability of selecting the ground truth option when the AI is wrong. Collectively, these results suggest that helpful examples and saliency maps improve human understanding of the AI in distinct and complementary ways. Errorbars represent 95% bootstrapped confidence intervals. All point estimates have confidence intervals, though some are too narrow to see clearly.

1.01(0.08), $z = -12.71$, $p < .0001$) and when the AI is wrong ($\beta = 0.33(0.05)$, $z = 7.35$, $p < .0001$). However, in contrast to the saliency maps, examples seem to be most helpful for unfamiliar trials when the AI is correct, see Figure 5 C. This effect may imply that the examples help participants

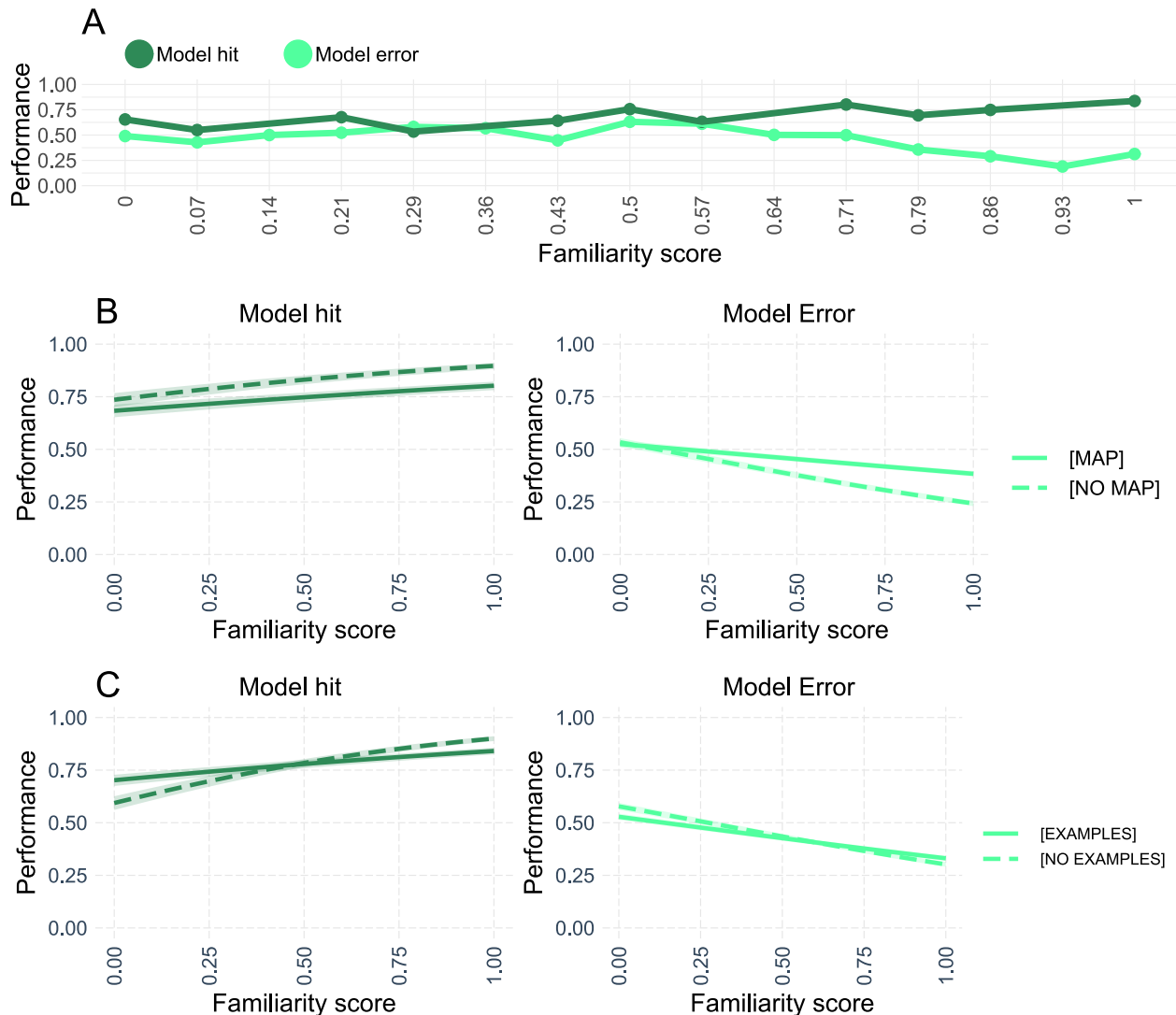


Figure 5: Familiarity score predicts human performance based on the full data set (631 participants; 94,582 observations). **(A)** Familiarity score is positively associated with correct predictions when the AI is right, but is negatively associated with correct prediction when the AI is wrong. This provides further evidence that participants project their own beliefs to model the AI. **(B)** Saliency maps decrease the impact of familiarity on participant judgements. For model hits this leads to decreased performance, whereas for model errors it leads to improved performance. This pattern provides further evidence that the saliency maps work by shifting participants away from using their first-order judgments to model the AI’s classifications. **(C)** Examples also decrease the impact of familiarity on participant judgements. For model hits this improves performance for unfamiliar items but decreases performance for familiar items, with the opposite pattern for model errors. These results suggest that examples are most beneficial for unfamiliar items when the model is correct. Errorbars represent 95% bootstrapped confidence intervals. All point estimates have confidence intervals, though some are too narrow to see clearly. Shaded areas represent analytic 95% confidence intervals.

develop a working representation of the unfamiliar categories, which they are otherwise lacking.

Discussion

Multiple strands of evidence from our results suggest that people default to belief-projection when reasoning about the AI’s decisions. Specifically, we find that participants in the control condition show higher sensitivity than specificity, and that this discrepancy becomes more extreme the more familiar participants are with the trial categories. Our results imply that such belief-projection can be mitigated by Bayesian Teaching. We find that examples selected to be helpful according to Bayesian Teaching help people to predict the AI’s decisions and are preferred over random examples or examples selected to be detrimental. The most compelling evidence that explanations mitigate belief projection is that the impact of familiarity on performance is reduced by explanations: explanations make participants more likely to catch AI mistakes on trials they themselves found easy. Beyond mitigating belief-projection, Bayesian Teaching predicts that examples can in fact be chosen to guide people to any target, including erroneous inference. Our results confirmed this prediction in that examples designed to mislead the participants reduced their performance below the no-intervention baseline.

Bayesian Teaching also gives a coherent framework for comparing and contrasting explanatory methods that hereto have been considered independent: explanation-by-examples and feature attribution. We apply Bayesian Teaching to study explanation-by-examples, a popular method for XAI that previously has lacked a sound theoretical footing. Explanation-by-examples has many strengths: it is model-agnostic, domain-general, and easy to use with other XAI methods. Viewed through a Bayesian Teaching lens, this method can be generalized to include feature attribution, another popular post-hoc method, by splitting each example into its component features (i.e. pixels in this study) and considering each pixel individually. When applied to images, such feature attribution on the pixel level generates saliency maps, which is arguably the most popular method for XAI in the image domain. The connection between feature attribution and pixel selection by Bayesian Teaching opens up the possibility to reinterpret all feature attribution methods (e.g., [51, 52]) as a form of teaching. By treating images and saliency maps as explanatory examples at different levels of granularity, we discover that the two explanations show complementary effects. Namely, example images are effective explanations for confirming the model’s correct classification of unfamiliar categories, and saliency maps are effective explanations for exposing the model’s incorrect classification of familiar categories.

The lack of a coherent theory is currently stifling XAI as methods are developed around technical innovations without any *a priori* hypothesis as to whether they are appropriate for the specific use case [53]. Bayesian Teaching both exposes this blind spot and offers a solution: effective explanation is a communication act which depends on a knowledgeable teacher, a good model of the learner and an awareness of the context in which inference takes place. Consequently, the framework encourages systematic evaluation of XAI interventions on these dimensions, and provides a way to systematically diagnose how interventions could be improved. In our study we show how such an evaluation applies to explanation-by-examples. We modeled both the explainer and explainee by a ResNet-50 architecture, focused on two contextual variables (familiarity and model correctness), and surfaced human inductive biases that are typically overlooked in XAI. Since the function of explanation is to shape the explainee’s inductive reasoning [54], we expect that dif-

ferent inductive biases call for different kinds of explanation. Our work confirms that different inductive biases can be mitigated by different explanation methods under different contexts, indicating a fruitful avenue for further XAI research. Furthermore, Bayesian Teaching exemplifies how XAI can be improved by considering links to other fields such as education and cognitive science. A balanced synergy between the social sciences and the more technical literature of AI is much needed, as XAI is simultaneously a machine-learning problem and a human-centered endeavor.

Methods

The objective of this study was to explore the effects of explanations, in the form of examples and saliency maps, on users' understanding of high-performing machine learning models (referred to as AI throughout the paper) in the domain of image classification. We probe users' understanding by a two-alternative-forced-choice (2AFC) task in which users are asked to predict the model's classification of a target image into one of two categories. Experimental conditions vary in terms of the information presented on the screen during each classification. The information presented differs along three dimensions: types of labels, types of examples, and types of saliency maps. All the examples and saliency maps are generated by the Bayesian Teaching framework. The predictive performance of the participant is captured by sensitivity, specificity, and accuracy.

The model to be explained

The machine learning model to be explained is a ResNet-50 model [38]. For this study, we used the pre-trained version of ResNet-50 in Keras with ImageNet weights. For the selection of saliency maps, the Bayesian Teaching framework expects the model to be able to make probabilistic inference on the image classification task presented in the ImageNet Large Scale Visual Recognition Challenge 2012 (ILSVRC2012). The ResNet-50 model has this capability, and we can use the ResNet-50 model without any modification. However, for the selection of examples, the Bayesian Teaching framework expects the model to be able to make probabilistic inference on the 2AFC task, and the ResNet-50 model is deterministic. We replace the fully-connected classification layer of the ResNet-50 model with a probabilistic linear discriminant analysis (PLDA) model [55]. This new PLDA layer is trained using a transfer-learning-like procedure. Training images were first passed through the ResNet-50 model and transformed into feature vectors. Then, the PLDA layer was fit to these feature vectors and the corresponding class labels following the algorithm presented in [55]. Using the training dataset *ImageNet 1K* from the ILSVRC2012 [44], this ResNet-50-PLDA model has a top-1 accuracy of 52.86% and a top-5 accuracy of 76.29%. For the actual experiment, we focused on a subset of 100 categories that include the most difficult, easiest, and most confusable categories (see the next subsection for details). Unless otherwise stated, all the model predictions used to design the experiment is based on the ResNet-50-PLDA model trained on the training data in only these 100 categories.

Stimuli selection

Each experiment consisted of 150 trials. For 50 of the trials, the predictions of the model (or the robot) matched the ground-truth labels of the target images. For the remaining 100, the model pre-

dictions did not match the ground-truth labels. We selected the target images and the classification categories based on the model’s confusion matrix, with the aim to cover a wide range of model behavior. First we calculated the ResNet-50-PLDA model’s confusion matrix on *ImageNet 1K*, which contains 1000 categories. Then, we randomly selected 25 categories from each of the following four subsets: the 100 categories on which the model was most accurate, the 100 categories that were most confusable with these most accurate categories, the 100 categories on which the model was least accurate, and the 100 categories that were most confusable with these least accurate categories. This resulted in 100 categories. We recorded the model’s predicted labels of all the training images in these 100 categories and marked all images for which the model predictions were also among these 100 categories.

From this subset where both the image and the top model prediction belonged to our 100 categories, we randomly sampled 50 images where the model prediction matched the ground truth labels and 100 images for which the model predictions did not match the ground-truth labels. For the 50 trials with correctly classified target images, the two classification options participants could choose from were the correct model-predicted category and one of the two most confusable categories (out of our 100 selected categories). Which one of the two most confusable categories was presented were selected randomly for each trial. For the 100 incorrectly classified trials the two classification options were simply the ground-truth category and the incorrect model prediction. This procedure resulted in a total of 83 unique categories used in the experiment (Supplementary Table T1). This number is smaller than 100 because not all confusable categories are unique and not all categories were kept during the random sampling. Figure 6 depicts the trial generating process. The pairs of categories used in the experiments are listed in Supplementary Table T2.

Experimental design

At the beginning of the experiment, participants were told that a robot has been trained to classify images but sometimes makes mistakes. They were asked to help by guessing how the robot will classify images. On each trial, a target image was displayed along with information about two categories, and the participants were asked to perform the 2AFC task by choosing which of the two categories they think the robot would classify the target image as.

The experimental conditions determined what information was presented during each trial and varied three dimensions: labels, examples, and saliency maps. Figure 1 shows a trial in the experimental condition with all the elements—labels, examples, and saliency maps—and describes how the conditions impact what elements are presented. More precisely, the conditions are characterized by five binary features: informative or generic labels, with or without examples, helpful or random examples (if present), with or without saliency maps, and blur or jet saliency maps (if present). The structured column and row labels of Table 1 show the naming conventions for the different conditions in terms of these features. Below, we provide more details on the conditions.

Specific or generic labels: Conditions with informative or generic labels are referred to as [SPECIFIC LABELS] and [GENERIC LABELS], respectively. In the [SPECIFIC LABELS] conditions, the English labels of the two categories (e.g., “Flagpole” and “Barn” in Figure 1) are given. In the [GENERIC LABELS] conditions, the two categories are named “Category A” and “Category B.”

With or without examples: Conditions with and without examples are referred to as [EXAMPLES] and [NO EXAMPLES], respectively. In the [EXAMPLES] conditions, two examples are sampled from each of the two categories to represent the category. Thus, five images—one target image

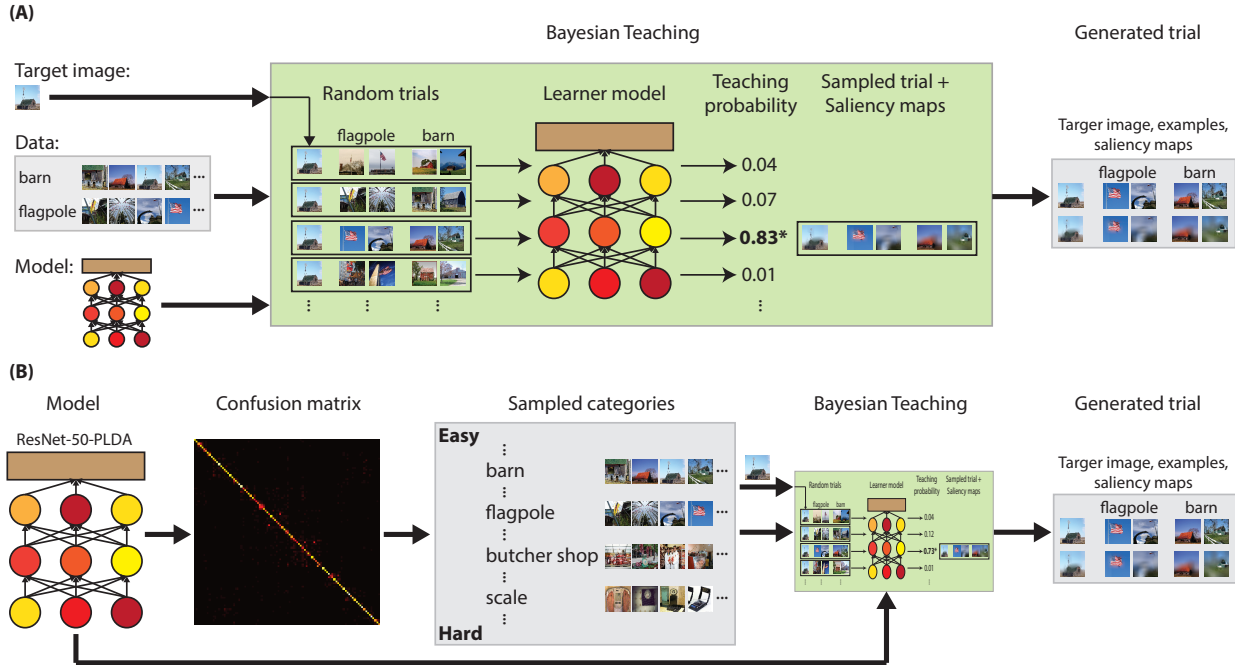


Figure 6: Flowchart of trial generation. **(A)**. Selection of examples and saliency maps with Bayesian Teaching. The inputs to Bayesian Teaching are: the model to be explained, data sets from two categories, and a target image that belongs to one of the two categories. The green box depicts the inner working of Bayesian Teaching. Random image pairs are selected from each of the input categories. Along with the target image, two sets of image pairs, one set from each category, are selected at random to form a trial. The learner model, which is set to have the same architecture as the input model, takes in a large number of random trials to produce the simulated learner performance (unnormalized teaching probabilities according to Equation 2). Here, a trial with high performance (probability) is selected, exemplifying the trial generation process in the [HELPFUL] condition. Saliency maps are generated for the target image and the four selected examples using Equation 5. The final output is a set of ten images: a target image, two examples selected from each of the two input categories, and the saliency maps of the above five images. **(B)**. Trial generation steps peripheral to Bayesian Teaching. Our model to be explained is a ResNet-50-PLDA trained on *ImageNet 1K*. A confusion matrix on the 1000 ImageNet categories was computed using the model. Using the confusion matrix, we sampled 25 categories where the model has high accuracy (the “Easy” categories), 25 categories where the model has low accuracy (the “Hard” categories), and the categories that are most confusable with the above 50 categories. To generate a trial, we select at random two categories from the 100 candidates mentioned above as well as a target image that belongs to one of the two selected categories. The model, the target image, and the data associated with the two categories are fed into Bayesian Teaching to produce a trial. See Methods for the full details.

and four example images—are on display in each trial in these conditions. In the [NO EXAMPLES] conditions, only the target image is shown.

Helpful or random examples: Conditions with the helpful examples and random examples are referred to as [HELPFUL] and [RANDOM], respectively. The selection of the examples are based on

the *simulated learner performance*, which is the numerator of the Bayesian Teaching probability, f_L . The simulated learner performance characterizes the probability that the four examples will lead a “learner model” to classify the target image as the ResNet-50-PLDA model would. The Bayesian Teaching probability and its numerator f_L are rigorously defined in Equations 1 and 2, respectively, in the subsection below called “Selection of examples with Bayesian Teaching.” In the [HELPFUL] conditions, the four examples are chosen such that $f_L > 0.8$. In the [RANDOM] conditions, the four examples are chosen such that the f_L values across the 150 trials are uniformly distributed over the five bins that evenly partition the [0,1] interval.

With or without saliency maps: Conditions with and without saliency maps are referred to as [MAP] and [NO MAP], respectively. A saliency map is an image mask that shows the contribution of each pixel to the model’s classification decision. Details on the generation of the saliency maps are provided in the subsection below called “Selection of saliency maps with Bayesian Teaching.” In the [MAP] conditions, a saliency map is shown for every image displayed. In the [NO MAP] conditions, no saliency map is shown.

Blur or jet saliency maps: Conditions with the blur saliency maps and jet saliency maps are referred to as [BLUR] and [JET], respectively. The two types of map differ only in the rendering of the mask but not in the generation of the mask. The jet saliency map renders the importance of each pixel by colors following the jet color map. In order of decreasing importance, the jet color map goes from red to green to blue. The jet color map, overlaid on an image with some level of transparency, is one of the most commonly used renderings of saliency maps. Two disadvantages of jet saliency maps are that the colors of the map can interfere with the colors of the image and that the unimportant regions remain visible to the user and can attract involuntary visual attention. For these reasons, we created the [BLUR] conditions in which the saliency maps are rendered by blurring the image. Furthermore, blurring is a more naturalistic visual effect than any color map masking because our visual system constantly experiences a large difference in visual acuity between our fovea and peripheral vision. The implementation details of both renderings are provided in the subsection below on saliency map selection.

Naming convention: As shown in Table 1, not all combinations of the five binary features are allowed. Conditions with generic labels and no examples are not tested because that would make the 2AFC task a game of pure guessing. Furthermore, conditions without examples cannot be paired with helpful or random examples, and conditions without saliency maps cannot be paired with blur or jet maps. This leaves a total of 15 experimental conditions.

The naming convention for the conditions is based on filter queries using the database structure presented in Table 1. To give a few examples: [HELPFUL] refers to the aggregate of the six conditions in columns 2 and 4; [MAP] refers to the aggregate of the 10 conditions in rows 2 and 3; [HELPFUL] & [BLUR] refers to the aggregate of the two conditions in row 2 column 2 and row 2 column 4; and [HELPFUL] & [BLUR] & [SPECIFIC LABELS] refers to the one condition in row 2 column 2.

Participants

The study protocol was approved by Rutgers University IRB. All research was performed in accordance with the approved study protocol. An IRB-approved consent page was displayed before the experiment. Informed consent was obtained from all participants. The experiment began after the participants gave consent.

656 participants (404 male, 249 female, 3 other) were recruited from Amazon Mechanical Turk and paid \$2.50 for completing the experiment, which took roughly 15 minutes to complete. The mean age of participants was 34.8 years (SD = 10.1), ranging from 18 to 72 years. The participants were randomly assigned to each condition, with the aim to obtain 36-40 participants per condition. 25 participants were excluded from analysis for completing the experiment too quickly (less than one second per trial), resulting in a final sample of 631 participants completing 150 trials each. The [NO EXAMPLES] conditions received twice the sample size of the other conditions, so that they would match the sample size of the [EXAMPLES] conditions, which had two distinct versions ([HELPFUL] and [RANDOM]). Table 1 shows the number participants in each of the 15 conditions.

The number of participants in every condition is shown in Table 1. All participants in the [HELPFUL] conditions experienced the same set of 150 trials, i.e., the same 150 combinations of target image, category pairs, and example images, but in randomized order. All participants in the [RANDOM] conditions experienced another set of 150 trials, also in randomized order. All the category pairs used are listed in Supplementary Table T2. Participants in the [NO EXAMPLES] condition experienced one of these two sets of trials, selected at random. Note that because there are no examples but only English labels in the [NO EXAMPLES] conditions, the two sets of trials are functionally equivalent.

Selection of examples with Bayesian Teaching

The goal of Bayesian Teaching is to select small subsets of the training data such that the inference made by a learner model using this small subset will be similar to the inference made by a target model using the entire training data. For this study, the target model is the ResNet-50-PLDA model trained on the 100 selected categories as described earlier. The inference task is to classify the target image among the 100 categories. The inference task of the learner model is the 2AFC image classification task presented in each trial. For the learner model, we search for an ideal-observer model [49, 50] that would capture the participant’s inference in the 2AFC task. A good candidate is the ResNet-50-PLDA because it is trained on human-labeled data and achieves high accuracy on predicting humans’ labelling behavior. This means that the target model and learner model share the same parameters (the ResNet-50 weights and PLDA parameters mentioned after Equation 3), and the use of Bayesian Teaching is focused on explaining the image classification inference based on roughly 100K training examples, i.e., all the training data in the 100 selected categories, with only four training examples, i.e., those selected to be displayed on each trial of the experiments in the [EXAMPLES] conditions.

We introduce some notation to define the Bayesian Teaching probability formally. The two categories that define the 2AFC task in each trial consist of the predicted category of the ResNet-50-PLDA model and an alternative category, which we denote by y^* and y , respectively. The two examples sampled from the model-predicted category are denoted by τ^{y^*} , and the two sampled from the alternative category are denoted by τ^y . Let the learner model be denoted by f_L and the target image be denoted by d^* . The Bayesian Teaching probability, P_T , is defined as the probability that the selected examples, τ^{y^*} and τ^y , will lead the learner model to classify the target image as the target model would. Mathematically, this probability can be expressed using Bayes’ rule as:

$$P_T(\tau^{y^*}, \tau^y \mid y^*, d^*) = \frac{f_L(y^* \mid \tau^{y^*}, \tau^y, d^*)}{\sum_{(\tau^{y^*}, \tau^y)' \in \Omega} f_L(y^* \mid (\tau^{y^*}, \tau^y)', d^*)}. \quad (1)$$

The sum in the denominator is over all possible candidate sets of the four examples. The set of all candidate sets is denoted by Ω . Equation 1 assumes a uniform prior over Ω so that the prior terms in the numerator and denominator cancel out. Technically, Ω is the Cartesian product of all possible pairings of images in the category y^* with all possible pairings of images in the category y , which is on the order of 10^{11} for the dataset in use. Our goal here is to select τ^{y^*} and τ^y such that f_L , the numerator of Equation 1, would provide good coverage of the full range of $[0,1]$. This would ensure the existence of valid examples for both the [RANDOM] and [HELPFUL] conditions. We found that the full range can usually be covered by forming a Cartesian product of 1000 random pairings from each category (10^6 combinations). In general, given a target value of f_L , one could use genetic algorithm [56] or other types of discrete optimization method to select the examples. To sample in proportion to P_T , one could use Markov Chain Monte Carlo and variational inference techniques [14, 57, 58]. These optimization and advanced inference methods would also be more efficient in the case that more than a few examples for each category is desired.

Using Bayes’ rule again, we express the learner model’s inference of the target image’s label given the target image and examples, the numerator in Equation 1, as

$$f_L(y^* | \tau^{y^*}, \tau^y, d^*) = \frac{f(d^* | \tau^{y^*})}{f(d^* | \tau^{y^*}) + f(d^* | \tau^y)}, \quad (2)$$

where $f(d^* | \tau^k)$ is the probability that the target image, d^* , belongs to the category from which the two example images, τ^k , are sampled. Under the PLDA model, one can write this probability in closed form as a normal distribution [21]:

$$f(d^* | \tau^k) = \mathcal{N} \left(u^* \left| \frac{\Psi}{2\Psi + \mathbf{I}}(u_1^k + u_2^k), \frac{\Psi}{2\Psi + \mathbf{I}} + \mathbf{I} \right. \right). \quad (3)$$

Here, u is an image transformed in two steps. First, the image is passed through ResNet-50 and transformed into a feature vector; then, this feature vector undergoes an affine transformation with shift vector \mathbf{m} and rotation and scaling matrix A to become u . Thus, in Equation 3, u^* is a transformed target image, and (u_1^k, u_2^k) are a pair of transformed examples sampled from category k . The quantities \mathbf{m} and A in the second transformation and the Ψ in Equation 3 are parameters of the PLDA model obtained by training on the images in the 100 selected categories. The precise definitions of these parameters and the training procedure are presented in Figure 2 in Ioffe’s PLDA paper [55].

To summarize this subsection, Equation 1 defines the Bayesian Teaching probability, and Equation 2 defines its numerator (simulated learner performance), f_L , used to select examples in the [EXAMPLES] conditions. A high f_L means that the selected examples will lead the model of the explainee (or learner) to classify the target image as the category predicted by the model to be explained with high probability. Conversely, a low f_L means that the selected examples will lead the learner model to classify the target image as the other category in the 2AFC with high probability. Note that f_L is trial specific, as this probability is a function of the target image, d^* , the model predicted label of the target image, y^* , and the four examples, (τ^{y^*}, τ^y) , which precisely define a trial.

Selection of saliency maps with Bayesian Teaching

A saliency map is an image mask that shows how important each pixel of the image is to the model’s inference. In the [MAP] conditions, we generate a saliency map for every image displayed. To generate a saliency map, one needs to specify a model, an inference task, and a definition of importance. We used ResNet-50 as the model and the classification of an image into the 1000 categories in *ImageNet 1K* as the inference task. Using the Bayesian Teaching framework, we define importance to be the probability that a mask, m , will lead the model to predict the image, d , to be in category, y , when the mask is applied to the image. This is expressed by Bayes’ rule as

$$Q_T(m | y, d) = \frac{g_L(y | d, m)p(m)}{\int_{\Omega_M} g_L(y | d, m)p(m)}. \quad (4)$$

Here, $g_L(y | d, m)$ is probability that the ResNet-50 model will predict the d masked by m to be y ; $p(m)$ is the prior probability of m ; and $\Omega_M = [0, 1]^{W \times H}$ is the space of all possible masks on an image with $W \times H$ pixels. The prior probability distribution $p(m)$ on m is a sigmoid-function squashed Gaussian process prior.

Instead of sampling the saliency maps directly from Equation 4, we find the expected saliency map for each image by Monte Carlo integration:

$$\begin{aligned} \mathbb{E}[M | y, d] &= \int_{\Omega_M} m Q_T(m | y, d) \\ &\approx \frac{\sum_{i=1}^N m_i g_L(y | d, m_i)}{\sum_{i=1}^N g_L(y | d, m_i)}, \end{aligned} \quad (5)$$

where m_i are samples from the prior distribution $p(m)$, and $N = 1000$ is the number of Monte Carlo samples used. To see why an expected map is desirable, imagine the following case. Suppose that an image contains 7 goldfish and its category is “goldfish.” In this case, a mask that reveals any one of the goldfish will have a high Q_T value. However, it is more desirable that the mask would reveal all the goldfish in the image. The expectation provides this by averaging the masks appropriately weighted by their Q_T values.

Now, we describe the step-by-step procedures for generating the saliency map for an image, d . First, d is resized to be 224-by-224 pixels, which is the size displayed in the experiments (Figure 1). A set of 1000 2D functions are sampled from a 2D Gaussian process (GP) with an overall variance of 100, a constant mean of -100 , and a radial-basis-function kernel with length scale 22.4 pixels in both dimensions. The sampled functions are evaluated on a 224-by-224 grid, and the function values are mostly in the range of $[-500, 300]$. A sigmoid function, $1/(1 + \exp(-x))$, is applied to the sampled functions to transform each of the function values, x , to be within the range $[0, 1]$. This results in 1000 masks. The mean of the GP controls how many effective zeros there are in the mask, and the variance of the GP determines how fast neighboring pixel values in the mask change from zero to one. The 1000 masks are the m_i ’s in Equation 5. We produce 1000 masked images by element-wise multiplying the image d with each of the masks. The term $g_L(y | d, m_i)$ is the ResNet-50’s predictive probability that the i^{th} masked image is in category y . Having obtained these predictive probabilities from ResNet-50, we average the 1000 masks according to Equation 5 to produce the saliency map of image d . If d is a target image, the y used to generate the saliency

map is the ResNet-50-PLDA model’s prediction. If d is an example, the y is the category from which the example is sampled.

In the [JET] conditions, the saliency maps are rendered in the Matplotlib package with the “jet” colormap and an alpha value of 0.4 and overlaid on the images (see Figure 1; images at the bottom row). In the [BLUR] conditions, a saliency map is rendered by blurring the image for which it is generated (Figure 1; images in the middle row). To generate the blur, each pixel value of a saliency map, z , is assigned a blurring window width, $w(z) = \text{ceil}(30/(1 + \exp(20z - 10)))$. The j^{th} pixel value of the rendered saliency map is the average pixel value of a patch of the original image, where the patch is w -by- w in size and centered on the j^{th} pixel of the original image. If the j^{th} pixel is close to an edge of the image, the patch becomes rectangular, and the average is over whichever pixel values that are inside the w -by- w sized window.

To conclude this subsection, we make a few final remarks. First, a PLDA layer is unnecessary in the generation of saliency maps because the ResNet-50 model is capable of generating the probabilities $g_L(y | d, m)$ in Equation 4. In contrast, the ResNet-50 model cannot be used directly to generate the probabilities $f_L(y^* | \tau^{y^*}, \tau^y, d^*)$ in Equation 1. Second, while the 2AFC task may be suitable for generating a saliency map for the target image, it cannot be used to generate saliency maps for the examples. This is the main reason that here we used the inference task of the image classification task that the ResNet-50 model is trained on. Lastly, Equation 5 is the same as Equation 5 in the RISE approach introduced by Petsiuk, Das, and Saenko [48], which presents a state-of-the art method for generating saliency maps. Our implementation and their implementation differ only in the way the individual masks are sampled. In our implementation, we sampled functions from a GP prior and turned them into masks by applying a sigmoid function. In [48], random binary matrices are first sampled and subsequently up-sampled to the desired mask size through bilinear interpolation. The expectation is done in the same way.

Familiarity coding

In addition to the splits by conditions presented in Table 1, analysis also rely on scores of human familiarity with the image categories. The familiarity of each of the [HELPFUL] and [RANDOM] trials was manually coded by 7 raters. Each rater was asked to code the trial as “familiar” if they thought they could correctly match the category labels to the images presented in that trial, and “unfamiliar” otherwise. A familiarity score for each pairing of categories was then constructed by assigning each raters judgements as 1 for familiar and 0 for unfamiliar, and computing the mean across raters. The 300 trials across the [HELPFUL] and [RANDOM] conditions resulted in 167 unique category pairings (counting the ordering of target versus other category), and their familiarity scores are presented in Supplementary Table T2.

Statistical analysis

Whenever we report testing how well participants predict the model classifications (performance), or how often their judgements correspond to the image ground truth (accuracy) we used hierarchical logistic regressions with random intercepts per participants and fixed effects for the remaining terms. For analyses of sensitivity and specificity analyses, we still used a logistic regression framework but only included trials corresponding to true positives and false negatives, or true negatives

and false positives, respectively. Sensitivity captures how well participants predict trials when the AI is correct, and specificity capture how well participants predict trials when the model is wrong.

To illustrate, *Bayesian Teaching improves predictive performance* used the following equations on the full set of trials, and on a subset of the trials to capture sensitivity and specificity respectively:

$$\Pr(\text{Performance}_i = 1) = \text{logit}^{-1}(\alpha_{j[i]} + \beta_1 \text{ExplanationCondition}_i + \epsilon_i), \text{ for } i = 1, \dots, I.$$

$$\text{logit}^{-1}(x) = \frac{\exp(x)}{1 + \exp(x)}$$

$$\alpha_j \sim N(U_j, \sigma_\alpha^2), \text{ for } j = 1, \dots, J.$$

where performance is a binary variable coded as 1 when participant correctly predict the AI classification and 0 otherwise, i is the observation index, j is the participant index. ExplanationCondition is a binary dummy variable coded as 1 if participants experienced heatmaps and helpful examples and 0 if they did not experience any explanations.

For the *Participants prefer helpful examples* section we compared three hierarchical logistic models: (A) An intercept only model that treated intercepts as nested within participants (B) an intercept only model that treated intercepts as nested within participants and conditions, (C) Model two, with an added fixed effect for the familiarity score. We then compared the negative log-likelihoods of these models to determine which best accounted for the observed data.

We evaluated whether *Bayesian Teaching can lead participants to both correct and incorrect inference* by predicting performance in the conditions containing examples by fitting three nested models:

$$\Pr(\text{Performance}_i = 1) = \text{logit}^{-1}(\alpha_{j[i]} + \beta_1 \text{ResNetAccuracy}_i + \epsilon_i), \text{ for } i = 1, \dots, I.$$

$$\Pr(\text{Performance}_i = 1) = \text{logit}^{-1}(\dots + \beta_2 \text{SimLearnerPerformance}_i + \epsilon_i), \text{ for } i = 1, \dots, I.$$

$$\Pr(\text{Performance}_i = 1) = \text{logit}^{-1}(\dots + \beta_3 \text{ModelCorrectness}_i + \beta_4 \text{ModelCorrectness}_i \text{ResNetAccuracy}_i + \beta_5 \text{ModelCorrectness}_i \text{SimLearnerPerformance}_i + \epsilon_i), \text{ for } i = 1, \dots, I.$$

where SimLearnerPerformance is the expected probability that the participant pick the same response as the target model, conditional on seeing the examples, and ModelCorrectness is a dummy variable coding if ResNet made a correct classification on this particular trial. We then compared the negative log likelihoods of these three models, and reported the coefficients of the best-fitting model (the interaction model).

In the *Bayesian Teaching improves performance through belief-mitigation* section we fitted four logistic hierarchical regression models to the full data. These models shared the following form:

$$\Pr(Y_i = 1) = \text{logit}^{-1}(\alpha_{j[i]} + \beta_1 \text{Familiarity}_i + \beta_2 \text{ResNetAccuracy}_i + \beta_3 \text{Examples}_i + \beta_4 \text{MAP}_i + \beta_5 \text{Labels}_i + \epsilon_i), \text{ for } i = 1, \dots, I. \quad (6)$$

where Familiarity is a proportion of raters who rated the trial categories as familiar, ResNetAccuracy, was the average ResNet accuracy for the target category, Examples, MAP and Labels where dummy variables that captured whether examples were shown, whether heatmaps were shown and whether category labels were informative or not, respectively.

These four models were distinguished based on whether the AI was correct or not and whether Y corresponded to whether the participant judgement matched the ground truth or matched the AI’s judgement. We fitted similar models to the [EXAMPLES] trials only, with the only difference being that the Examples term, that previously had captured whether examples were present was replaced with a dummy variable that captured whether the examples presented were helpful or not. Finally, we fitted two more models predicting participant performance from the full data. These are similar to Equation 6, but added two additional interaction terms:

$$\Pr(Y_i = 1) = \text{logit}^{-1}(\dots + \beta_6 \text{MAP}_i \text{Familiarity}_i + \beta_7 \text{Examples}_i \text{Familiarity}_i + \epsilon_i), \text{ for } i = 1, \dots, I.$$

Coefficient tables for these models can be found in Supplementary Tables T3. All hierarchical logistic regression models were fitted using the lme4 package (1.1-23) [59] in R version 4.0.3.

Data availability

Raw experimental data and analysis code will be deposited at TBA upon publication.

Acknowledgments

This material is based on research sponsored by the Air Force Research Laboratory and DARPA under agreement number FA8750-17-2-0146 to P.S. and S.Y. The U.S. Government is authorized to reproduce and distribute reprints for Governmental purposes notwithstanding any copyright notation thereon.

This work was also supported by DoD grant 72531RTREP, NSF SMA-1640816, NSF MRI 1828528 to PS. The methods described herein are covered under Provisional Application No. 62/774,976.

Author contributions

S.C.-H.Y., W.K.V., R.B.S, and P.S. conceived and designed the experiments. W.K.V. and S.C.-H.Y. conducted the experiments. R.B.S. and S.C.-H.Y. prepared materials for the experiments. T.F., W.K.V., and S.C.-H.Y. analyzed the data. S.C.-H.Y., T.F., W.K.V., R.B.S, and P.S. wrote the paper.

Competing interests

The authors declare no competing interests.

References

- [1] Finale Doshi-Velez, Mason Kortz, Ryan Budish, Chris Bavitz, Sam Gershman, David O’Brien, Kate Scott, Stuart Schieber, James Waldo, David Weinberger, et al. Accountability of ai under the law: The role of explanation. *arXiv preprint arXiv:1711.01134*, 2017.

- [2] Pranav Rajpurkar, Jeremy Irvin, Kaylie Zhu, Brandon Yang, Hershel Mehta, Tony Duan, Daisy Ding, Aarti Bagul, Curtis Langlotz, Katie Shpanskaya, et al. Chexnet: Radiologist-level pneumonia detection on chest x-rays with deep learning. *arXiv preprint arXiv:1711.05225*, 2017.
- [3] Andre Esteva, Brett Kuprel, Roberto A Novoa, Justin Ko, Susan M Swetter, Helen M Blau, and Sebastian Thrun. Dermatologist-level classification of skin cancer with deep neural networks. *Nature*, 542(7639):115, 2017.
- [4] European Commission. 2018 reform of eu data protection rules. https://ec.europa.eu/commission/sites/beta-political/files/data-protection-factsheet-changes_en.pdf, 2018.
- [5] Diane Coyle and Adrian Weller. ?explaining? machine learning reveals policy challenges. *Science*, 368(6498):1433–1434, 2020.
- [6] Brenden M Lake, Tomer D Ullman, Joshua B Tenenbaum, and Samuel J Gershman. Building machines that learn and think like people. *Behavioral and brain sciences*, 40, 2017.
- [7] John Stuart Mill. *A system of logic, ratiocinative and inductive: Being a connected view of the principles of evidence and the methods of scientific investigation*. Longmans, green, and Company, 1889.
- [8] Paul Bloom. *How children learn the meanings of words*. MIT press, 2002.
- [9] Fei Xu and Joshua B Tenenbaum. Word learning as bayesian inference. *Psychological review*, 114(2):245, 2007.
- [10] Brenden M Lake and Steven T Piantadosi. People infer recursive visual concepts from just a few examples. *Computational Brain & Behavior*, 3(1):54–65, 2020.
- [11] Michelene TH Chi, Miriam Bassok, Matthew W Lewis, Peter Reimann, and Robert Glaser. Self-explanations: How students study and use examples in learning to solve problems. *Cognitive science*, 13(2):145–182, 1989.
- [12] Vincent AWMM Alevan. *Teaching case-based argumentation through a model and examples*. Citeseer, 1997.
- [13] Liz Bills, Tommy Dreyfus, John Mason, Pessia Tsamir, Anne Watson, and Orit Zaslavsky. Exemplification in mathematics education. In *Proceedings of the 30th Conference of the International Group for the Psychology of Mathematics Education*, volume 1, pages 126–154. ERIC, 2006.
- [14] Jianbo Chen, Le Song, Martin Wainwright, and Michael Jordan. Learning to explain: An information-theoretic perspective on model interpretation. In *International Conference on Machine Learning*, pages 882–891, 2018.
- [15] Baxter S Eaves Jr, April M Schweinhart, and Patrick Shafto. Tractable bayesian teaching. In *Big Data in Cognitive Science*, pages 74–99. Psychology Press, 2016.

- [16] Mark K Ho, Michael Littman, James MacGlashan, Fiery Cushman, and Joseph L Austerweil. Showing versus doing: Teaching by demonstration. In *Advances in neural information processing systems*, pages 3027–3035, 2016.
- [17] Lisa Anne Hendricks, Ronghang Hu, Trevor Darrell, and Zeynep Akata. Generating counterfactual explanations with natural language. *arXiv preprint arXiv:1806.09809*, 2018.
- [18] Atsushi Kanehira and Tatsuya Harada. Learning to explain with complementary examples. In *Proceedings of the IEEE Conference on Computer Vision and Pattern Recognition*, pages 8603–8611, 2019.
- [19] Been Kim, Cynthia Rudin, and Julie A Shah. The bayesian case model: A generative approach for case-based reasoning and prototype classification. In *Advances in Neural Information Processing Systems*, pages 1952–1960, 2014.
- [20] Been Kim, Rajiv Khanna, and Oluwasanmi O Koyejo. Examples are not enough, learn to criticize! criticism for interpretability. In *Advances in Neural Information Processing Systems*, pages 2280–2288, 2016.
- [21] Wai Keen Vong, Ravi B. Sojitra, Anderson Reyes, Scott Cheng-Hsin Yang, and Patrick Shafto. Bayesian teaching of image categories. In *Proceedings of the 40th Annual Conference of the Cognitive Science Society*, 2018.
- [22] Tongzhou Wang, Jun-Yan Zhu, Antonio Torralba, and Alexei A Efros. Dataset distillation. *arXiv preprint arXiv:1811.10959*, 2018.
- [23] Pang Wei Koh and Percy Liang. Understanding black-box predictions via influence functions. In *Proceedings of the 34th International Conference on Machine Learning-Volume 70*, pages 1885–1894. JMLR. org, 2017.
- [24] Nicolas Papernot and Patrick McDaniel. Deep k-nearest neighbors: Towards confident, interpretable and robust deep learning. *arXiv preprint arXiv:1803.04765*, 2018.
- [25] Chih-Kuan Yeh, Joon Kim, Ian En-Hsu Yen, and Pradeep K Ravikumar. Representer point selection for explaining deep neural networks. In *Advances in Neural Information Processing Systems*, pages 9291–9301, 2018.
- [26] Yash Goyal, Ziyang Wu, Jan Ernst, Dhruv Batra, Devi Parikh, and Stefan Lee. Counterfactual visual explanations. *arXiv preprint arXiv:1904.07451*, 2019.
- [27] Rich Caruana, Hooshang Kangarloo, JD Dionisio, Usha Sinha, and David Johnson. Case-based explanation of non-case-based learning methods. In *Proceedings of the AMIA Symposium*, page 212. American Medical Informatics Association, 1999.
- [28] Mark T Keane and Eoin M Kenny. How case-based reasoning explains neural networks: A theoretical analysis of xai using post-hoc explanation-by-example from a survey of ann-cbr twin-systems. In *International Conference on Case-Based Reasoning*, pages 155–171. Springer, 2019.

- [29] Scott Cheng-Hsin Yang and Patrick Shafto. Explainable artificial intelligence via bayesian teaching. *NIPS 2017 workshop on Teaching Machines, Robots, and Humans.*, 2017.
- [30] Tim Miller. Explanation in artificial intelligence: Insights from the social sciences. *Artificial Intelligence*, 2018.
- [31] Lee S Shulman. Those who understand: Knowledge growth in teaching. *Educational researcher*, 15(2):4–14, 1986.
- [32] Helen L Chick. Teaching and learning by example. *Mathematics: Essential research, essential practice*, 1:3–21, 2007.
- [33] Patrick Shafto, Noah D. Goodman, and Thomas L. Griffiths. A rational account of pedagogical reasoning: Teaching by, and learning from, examples. *Cognitive Psychology*, 71:55–89, 2014.
- [34] Baxter S Eaves Jr, Naomi H Feldman, Thomas L Griffiths, and Patrick Shafto. Infant-directed speech is consistent with teaching. *Psychological review*, 123(6):758, 2016.
- [35] Scott Cheng-Hsin Yang, Yue Yu, Arash Givchi, Pei Wang, Wai Keen Vong, and Patrick Shafto. Optimal cooperative inference. In *International Conference on Artificial Intelligence and Statistics*, pages 376–385, 2018.
- [36] Oisín Mac Aodha, Shihan Su, Yuxin Chen, Pietro Perona, and Yisong Yue. Teaching categories to human learners with visual explanations. In *Proceedings of the IEEE Conference on Computer Vision and Pattern Recognition*, pages 3820–3828, 2018.
- [37] Yuxin Chen, Oisín Mac Aodha, Shihan Su, Pietro Perona, and Yisong Yue. Near-optimal machine teaching via explanatory teaching sets. In *International Conference on Artificial Intelligence and Statistics*, pages 1970–1978, 2018.
- [38] Kaiming He, Xiangyu Zhang, Shaoqing Ren, and Jian Sun. Deep residual learning for image recognition. In *Proceedings of the IEEE Conference on Computer Vision and Pattern Recognition*, pages 770–778, 2016.
- [39] Tor Tarantola, Dharshan Kumaran, Peter Dayan, and Benedetto De Martino. Prior preferences beneficially influence social and non-social learning. *Nature communications*, 8(1):1–14, 2017.
- [40] Shinsuke Suzuki, Emily LS Jensen, Peter Bossaerts, and John P O’Doherty. Behavioral contagion during learning about another agent’s risk-preferences acts on the neural representation of decision-risk. *Proceedings of the National Academy of Sciences*, 113(14):3755–3760, 2016.
- [41] Chris L Baker, Rebecca Saxe, and Joshua B Tenenbaum. Action understanding as inverse planning. *Cognition*, 113(3):329–349, 2009.
- [42] Branden J Bio, Taylor W Webb, and Michael SA Graziano. Projecting one’s own spatial bias onto others during a theory-of-mind task. *Proceedings of the National Academy of Sciences*, 115(7):E1684–E1689, 2018.

- [43] Ágnes Melinda Kovács, Ernő Téglás, and Ansgar Denis Endress. The social sense: Susceptibility to others? beliefs in human infants and adults. *Science*, 330(6012):1830–1834, 2010.
- [44] Olga Russakovsky, Jia Deng, Hao Su, Jonathan Krause, Sanjeev Satheesh, Sean Ma, Zhiheng Huang, Andrej Karpathy, Aditya Khosla, Michael Bernstein, Alexander C. Berg, and Li Fei-Fei. ImageNet Large Scale Visual Recognition Challenge. *International Journal of Computer Vision (IJCV)*, 115(3):211–252, 2015.
- [45] Russell W Clement and Joachim Krueger. The primacy of self-referent information in perceptions of social consensus. *British Journal of Social Psychology*, 39(2):279–299, 2000.
- [46] Stefano Palminteri, Germain Lefebvre, Emma J Kilford, and Sarah-Jayne Blakemore. Confirmation bias in human reinforcement learning: Evidence from counterfactual feedback processing. *PLoS computational biology*, 13(8):e1005684, 2017.
- [47] Doris Pischedda, Stefano Palminteri, and Giorgio Coricelli. The effect of counterfactual information on outcome value coding in medial prefrontal and cingulate cortex: from an absolute to a relative neural code. *Journal of Neuroscience*, 40(16):3268–3277, 2020.
- [48] Vitali Petsiuk, Abir Das, and Kate Saenko. RISE: Randomized Input Sampling for Explanation of Black-box Models. *arXiv preprint*, 2018.
- [49] Wilson S Geisler. Ideal observer analysis. *The visual neurosciences*, 10(7):12–12, 2003.
- [50] Wilson S Geisler. Contributions of ideal observer theory to vision research. *Vision research*, 51(7):771–781, 2011.
- [51] Marco Tulio Ribeiro, Sameer Singh, and Carlos Guestrin. “why should i trust you?”: Explaining the predictions of any classifier. In *Proceedings of the 22nd ACM SIGKDD international conference on knowledge discovery and data mining*, pages 1135–1144. ACM, 2016.
- [52] Scott M Lundberg and Su-In Lee. A unified approach to interpreting model predictions. In *Advances in Neural Information Processing Systems*, pages 4765–4774, 2017.
- [53] Finale Doshi-Velez and Been Kim. Towards a rigorous science of interpretable machine learning. *arXiv preprint arXiv:1702.08608*, 2017.
- [54] Tania Lombrozo. The structure and function of explanations. *Trends in cognitive sciences*, 10(10):464–470, 2006.
- [55] Sergey Ioffe. Probabilistic linear discriminant analysis. In *European Conference on Computer Vision*, pages 531–542. Springer, 2006.
- [56] Thomas Back. *Evolutionary algorithms in theory and practice: evolution strategies, evolutionary programming, genetic algorithms*. Oxford university press, 1996.
- [57] Heikki Haario, Marko Laine, Antonietta Mira, and Eero Saksman. Dram: efficient adaptive mcmc. *Statistics and computing*, 16(4):339–354, 2006.

- [58] Dougal Maclaurin and Ryan Prescott Adams. Firefly monte carlo: Exact mcmc with subsets of data. In *Twenty-Fourth International Joint Conference on Artificial Intelligence*, 2015.
- [59] Douglas Bates, Deepayan Sarkar, Maintainer Douglas Bates, and L Matrix. The lme4 package. *R package version*, 2(1):74, 2007.

Supplementary information: Mitigating belief projection in explainable artificial intelligence via Bayesian Teaching

Supplementary Table T1

ImageNet categories used in the experiment. The 83 categories and their corresponding ResNet accuracy are given in this table. The accuracy scores are computed on the test set of *ImageNet 1K* over the 100 selected categories described in Methods. See separate csv file.

Supplementary Table T2

. The table lists all 167 unique pairs of categories used in the experiment along with each pair's familiarity score. See separate csv file.

Supplementary Tables T3

Coefficient tables for the 15 regression models reported in the main text. See separate excel file.

Supplementary Discussion D1: Participants prefer helpful examples

Methods

To test the subjective preference for helpful versus unhelpful or random examples, we use a different task. In a trial of this task, we presented a target image, its category, and two sets of example pairs for that category. The participants were asked to select which pair they think influenced the AI's classification more. Note that this experiment is different from the 2AFC experiment described previously in that there is only one category and the decision is between teaching sets.

Helpful examples are chosen to be the teaching examples for the target category in trials where $f_L > 0.8$. Likewise, unhelpful examples are chosen to be the examples for the target category in trials where $f_L < 0.2$. On average, these examples are expected to be helpful or detrimental regardless of what the other category is; thus, they can be approximated as examples that aim to maximize or minimize the marginal teaching probability. We extracted 67 target images that have both helpful examples and unhelpful examples. Given a target image's category, random examples are simply random samples from the training images in *ImageNet 1K* that are not the target image or the helpful examples.

80 participants (25 male, 54 female, 1 other) were recruited from Amazon Mechanical Turk and paid \$1.00 for completing the experiment, which took roughly 5 minutes to complete. The participants were randomly assigned to each of the two conditions (helpful-vs-unhelpful and helpful-vs-random) with 40 in each condition. The mean age of participants was 36.7 years (SD = 10.5), ranging from 16 to 68 years. 6 participants were excluded from analysis for completing the experiment too quickly (less than one second per trial), resulting in a final sample of 74 participants.

The study protocol was approved by Rutgers University IRB. All research was performed in accordance with the approved study protocol. An IRB-approved consent page was displayed before the experiment. Informed consent was obtained from all participants. The experiment began after the participants gave consent.

Results

We wanted to evaluate whether participants preferred informative to uninformative and misleading examples. To test this, we ran a second study where participants chose between helpful examples versus random examples ($n=37$) or versus unhelpful examples ($n=37$). The helpfulness of the examples is determined by Bayesian Teaching. The helpful examples are chosen to best represent the target category by maximizing the marginal teaching probability; random examples are uniformly randomly sampled from the target category; and unhelpful examples are chosen to mislead the learner to infer any other category by minimizing the marginal teaching probability. The marginal teaching probability is the probability that a set of examples will lead the explainee model to infer the target category compared to any other category in a 2AFC task (see Methods for more details).

Participants showed a small but reliable preference for helpful relative to random examples (53.05% [95% CI = 51.08% - 55.01%], $z=3.03$, $p = .002$) and a substantial preference for helpful versus to unhelpful examples (64.14% [95% CI = 61.68% - 66.59%], $z=10.95$, $p < .0001$). These two conditions were reliably different ($\chi^2 = 36.94$, $p < .0001$), implying that the Bayesian Teacher

is not only capable of selecting helpful examples, but can also select examples that are actively confusing (see Figure D1-1). As this pattern of preferences matches our predictions as stated in the introduction, a natural next steps is to evaluate whether these preferences are particularly pronounced for unfamiliar examples, as hypothesised. We found that participants were more likely to prefer helpful examples when the choice categories were unfamiliar to them ($\beta = -0.57(0.08)$, $z = -7.02$, $p < .0001$), irrespective of whether helpful examples were contrasted with random or unhelpful examples.

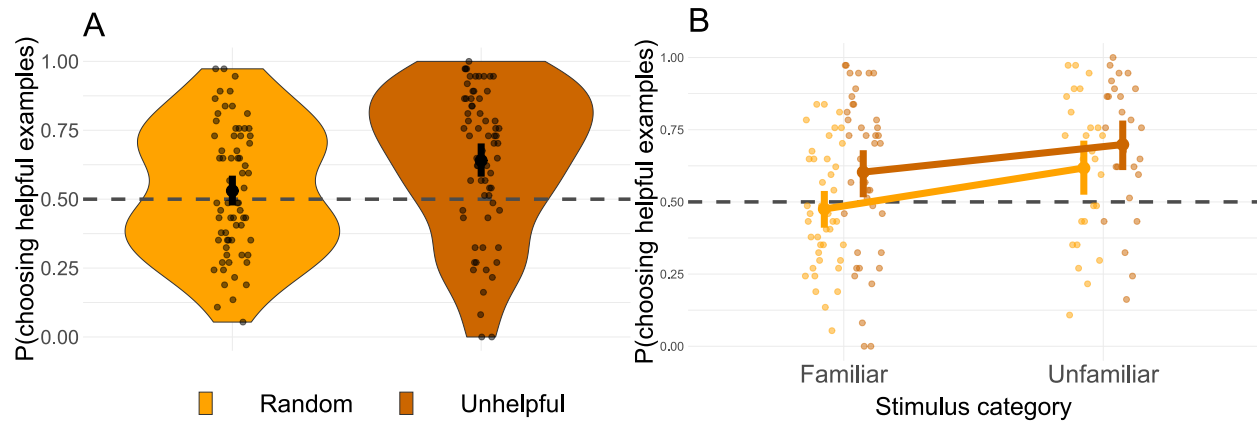


Figure D1-1: The popularity of helpful examples. **(A)**. The probability that a participant chose helpful examples over random (37 participants; 2479 observations), or unhelpful examples (37 participants; 2479 observations) respectively. **(B)**. The less familiar participants are with the stimulus categories, the more they prefer helpful examples. Familiarity ratings were continuous in the analyses reported in the main text, but are dichotomized here for visual clarity. Each transparent point represents the average probability across participants for one specific stimulus pair. Solid points represent the mean across all stimulus pairs. Error bars signify 95% bootstrapped confidence intervals.

Supplementary Discussion D2: Analysing MAP conditions separately

In the main text we combined the two MAP conditions in our analyses. To show that this decision did not meaningfully impact our conclusions we repeat the same analyses with [JET] and [BLUR] as separate predictors here. We ran hierarchical logistic regressions on the complete dataset predicting performance from the interventions ([SPECIFIC-LABELS] vs [GENERIC-LABELS], [BLUR] vs [JET] vs [NO MAP], and [EXAMPLES] vs [NO EXAMPLES]), while controlling for ResNet-50-PLDA accuracy and familiarity ratings.

[BLUR] improves performance when the AI is wrong ($\beta = 0.43(0.03)$, $z = 12.27$, $p < .0001$), as do [JET] ($\beta = 0.43(0.03)$, $z = 12.34$, $p < .0001$). However, the masks reduce performance (to a lesser extent) when the AI is correct, both for [BLUR] ($\beta = -0.49(0.08)$, $z = -6.06$, $p < .0001$) and for [JET] ($\beta = -0.62(0.08)$, $z = -7.76$, $p < .0001$), see Figure D2-1. In both cases, the saliency maps reduced the first order-accuracy of the participants. [BLUR] AI correct: $\beta = -0.49(0.08)$, $z = -6.05$, $p < .0001$, AI wrong: $\beta = -0.43(0.03)$, $z = -12.27$, $p < .0001$; [JET] AI correct: $\beta = -0.62(0.08)$, $z = -7.76$, $p < .0001$, AI wrong: $\beta = -0.43(0.03)$, $z = -12.34$, $p < .0001$. This reduction in first-order accuracy means that they were less likely to believe that the AI judgements matched the ground truth of the image. This in turn implies that the saliency maps encourage participants to consider that the AI might be mistaken. This interpretation assumes that participants know the ground truth for most of the trials, which seems plausible given the familiarity ratings.

The familiarity ratings capture the ease of the discrimination task in that they are higher for trials involving categories that humans are familiar with. We can use these ratings to further explore whether participants project their own beliefs onto the AI. Specifically, if humans use their first-order classifications to model the AI, familiarity should positively correlate with predictive performance when the AI is correct, but negatively correlate with predictive performance when the AI is wrong. This is indeed what we find: participants are more likely to accurately predict AI classifications when they are familiar with the item categories and the AI is correct ($\beta = 1.10(0.04)$, $z = 29.28$, $p < .0001$), but they are less likely to correctly predict AI errors ($\beta = -0.92(0.02)$, $z = -42.82$, $p < .0001$). In other words, participants are more likely to assume that the AI gets it right for trials that they themselves find easy.

Previously we showed that saliency maps improved prediction accuracy on trials when the AI was wrong. We suggested that this might be explained by saliency maps helping participants distinguish between their first-order judgements of the ground truth and their performance on predicting the model classification. This can be evaluated directly by testing whether the impact of the familiarity ratings on classification accuracy are attenuated by the saliency maps (see Figure D2-1). In other words, if participants are more likely to predict that the AI is correct on trials that they themselves find easy, and the saliency maps work by helping people realise that the AI use different decision-processes, the saliency maps should make participants more willing to consider that the AI is wrong for trials they themselves find easy. This is what we find, see Figure D2-1). Specifically, the presence of [BLUR] maps reduces the positive impact of familiarity on second-order accuracy when the AI is correct ($\beta = -0.61(0.09)$, $z = -6.67$, $p < .0001$) and the same is true for [JET] maps ($\beta = -0.44(0.09)$, $z = -4.87$, $p < .0001$). Conversely, saliency maps reduce the negative impact of familiarity on second-order accuracy when the AI is wrong, for both [BLUR] ($\beta = 0.74(0.05)$, $z = 13.95$, $p < .0001$) and [JET] ($\beta = 0.67(0.05)$, $z = 12.73$, $p < .0001$). Collectively

these results suggest that the presence of saliency maps help participants model the AI as an agent with distinct beliefs that may conflict with their own.



Figure D2-1: Masks improve human performance for identifying model errors, and reduce performance for identifying model hits, irrespective of how they are presented. All subplots are based on the entire data set, comparing [JET] and [BLUR] and [NO MAP] conditions (631 participants; 94,582 observations). **(A)**. The saliency maps improve performance for trials when the AI is wrong but reduce performance when the AI is correct. **(B)**. The saliency maps make people less likely to classify the target image to align with the ground truth, independent of AI accuracy. Together, A & B imply that the saliency maps help people to consider that the AI might make mistakes. **(C)** Saliency maps decrease the impact of familiarity on participant judgements. For model hits this leads to decreased performance, whereas for model errors it leads to improved performance. This pattern provides further evidence that the saliency maps work by shifting participants away from using their first-order judgments to model the AI classifications. Collectively these figures suggest that [JET] and [BLUR] have very similar impacts on participant judgements. Errorbars represent 95% bootstrapped confidence intervals. All point estimates have confidence intervals, though some are too narrow to see clearly. Shaded areas represent analytic 95% confidence intervals.

Supplementary Figure F1: The relationship between ResNet Accuracy and participant performance in the control condition

Focusing exclusively on the control trials, we see that ResNet accuracy is positively associated with human predictive performance when the AI is wrong ($\beta = 0.81(0.11)$, $z = 6.95$, $p < .0001$), but even more so when the AI is correct ($\beta = 0.92(0.23)$, $z = 3.96$, $p < .0001$).

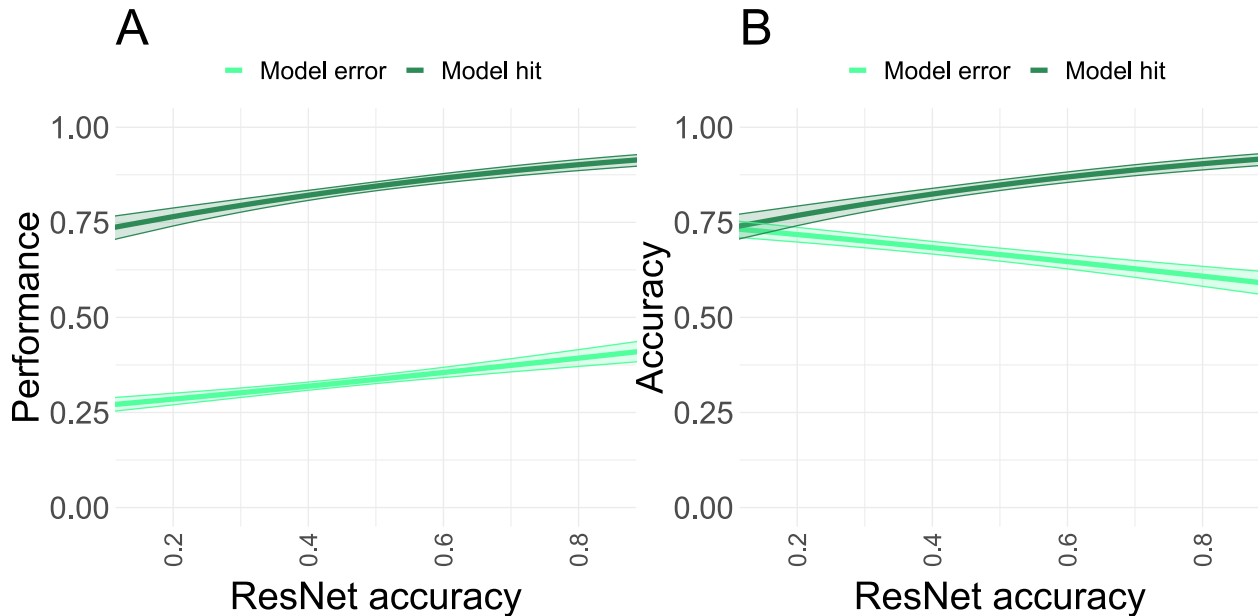


Figure F1: **(A)** ResNet accuracy is positively associated with human performance during the control condition both for trials when the AI is correct and when the AI is wrong. However, the base rate human performance is much higher when the AI is correct. **(B)** The probability that the participant judgement corresponds to the ground truth is positively associated with ResNet accuracy when the model is correct, but negatively associated with ResNet accuracy when the model is wrong. Masks improve human performance for identifying model errors, and reduce performance for identifying model hits, irrespective of how they are presented. Both subplots are based on the control trials only (76 participants; 11,394 observations). Shaded areas represent analytic 95% confidence intervals.